

Sound-resonance hydrogen sensor

[Shuxiang Dong](#), [Feiming Bai](#), [JieFang Li](#), and [Dwight Viehland](#)

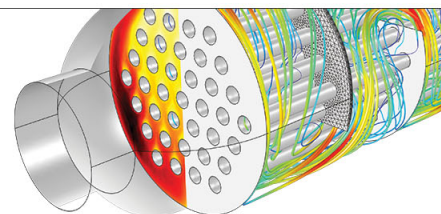
Citation: [Applied Physics Letters](#) **82**, 4590 (2003); doi: 10.1063/1.1586994

View online: <http://dx.doi.org/10.1063/1.1586994>

View Table of Contents: <http://scitation.aip.org/content/aip/journal/apl/82/25?ver=pdfcov>

Published by the [AIP Publishing](#)

Over **700** papers &
presentations on
multiphysics simulation



VIEW NOW ►

 COMSOL

Sound-resonance hydrogen sensor

Shuxiang Dong,^{a)} Feiming Bai, JieFang Li, and Dwight Viehland
Materials Science and Engineering, Virginia Tech, Blacksburg, Virginia 24061

(Received 28 February 2003; accepted 28 April 2003)

A hydrogen sensor is reported in which a small piezoelectric-sound-resonance-cavity (PSRC) is used as the sensing element. Detection utilizes sound resonance and acoustic property differences between H₂ and air as a sensing mechanism. Changes in H₂ concentration result in a shift of the sound-resonance state of the PSRC. Preliminary experiments have demonstrated a sensitivity limit of 8 ppm, a fast response time ~ 1.5 second, and detection capabilities over a broad concentration range $10^{-5} < n < 0.2$. © 2003 American Institute of Physics. [DOI: 10.1063/1.1586994]

Gas sensors have been developed for a wide range of air-borne hazardous species, including flammable and toxic gases. Current solid-state gas sensors can be classified into three types based upon their sensing mechanism,^{1–6} including: (i) Semiconducting ceramics that use electronic conductivity (i.e., surface resistivity), (ii) solid electrolytes that use ionic conductivity, and (iii) solid-state dielectrics that use capacitance. The response times of these solid-state gas sensors are quite slow, dependent upon the equilibrium adsorption of gases onto solid surfaces. They often can detect the presence of a gas; however, they have compromised signal sensitivity to gas concentrations and reduced response times. They are not useful for rapid quantitative detection over a significant concentration range.

Also, solid-state ceramic gas sensors often require relatively high operational temperatures (150 to 500 °C), making them unsuitable for the detection of flammable gases and liquids. As an alternative, polymer-based gas sensors have been developed which use an admittance (capacitance and conductance) detection method.^{7,8} These types of solid-state gas sensors can be operated at room temperature. However, they have very slow response times, as the admittance changes are dependent upon adsorption of gas species onto polymer surfaces. Again, they lack rapid, quantitative detection capabilities.

There are other alternative solid-state sensors based upon (i) optical/photoacoustic properties, (ii) surface acoustic waves, (iii) palladium mesowire, (iv) piezoelectric, and (v) microelectromechanical systems (semiconducting) mechanisms. The main problems associated with these types of sensors are a H₂ saturation problem, and/or a very low operational temperature (i.e., photoacoustic gas sensor).^{9–17}

Clearly, other types of gas sensors are needed which have enhanced sensitivity, quicker response times, and quantitative detection capabilities over a wider concentration range for H₂ leak detection, such as health monitoring of aerospace fuel tanks, in which H₂ is a known detected gas. The acoustic properties of gases have been used as a sensing mechanism for air pollutions¹⁸ and humidity detection (using surface acoustic wave).¹⁹ We will show that it is also a good sensing mechanism for H₂ detection, as there are significant

differences in the sound speeds, mass densities, and acoustic impedances between H₂ and air.

Figure 1 illustrates the concept of a PSRC sensor. Two disk-type piezoelectric thin layers are placed at each end of a small cavity (cylindrical type), in which one piezoelectric film has a center hole. One of the piezoelectric films is used to produce a bending vibration under a small applied ac voltage signal (V_{ac}), forcing the air in the cavity to vibrate. At resonance, the air will be in a standing wave sound resonance state. The second piezoelectric element at the opposite end of the cavity acts as a sensing element, capable of monitoring the changes of both the acoustic intensity (ΔI) and frequency of the standing wave (Δf). The piezoelectric sensor will produce a voltage signal (V_s) and phase signal (P_s) which are proportional to ΔI and Δf .

The resonance frequency of a cavity containing air of a nominal composition is

$$f_0 = K C_{air}, \quad (1)$$

where K is a geometric parameter related to the structure and size of the cavity, and C_{air} is air sound velocity. When H₂ enters the cavity, supposing the H₂ concentration percentage to be n (n is a small quantity), and the air concentration percentage to be $(1-n)$, the average density of the air and hydrogen gas can be estimated as $\bar{\rho} = n\rho_{H_2} + (1-n)\rho_{air}$. According to ideal gas laws, the average sound velocity of the air and hydrogen gas is $\bar{C} \approx C_{air}/\sqrt{1-n}$ (when $n \ll 1$). As a

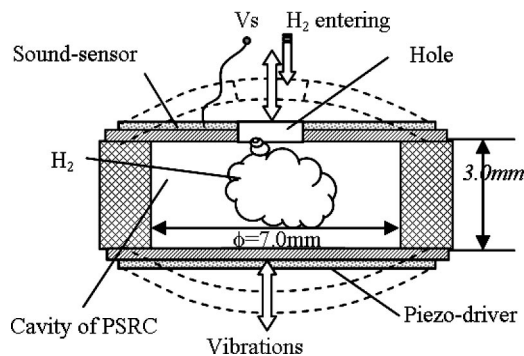


FIG. 1. Illustration of the concept of the PSRC sensor. The bottom piezo-driver produces a standing wave sound-resonance state in the cavity of PSRC. The top sound-sensor senses the changes of both acoustic intensity (I) and frequency (f_0) of the standing wave caused by H₂ gas.

^{a)}Electronic mail: sdong@vt.edu

result, the resonance frequency shift and acoustic characteristic impedance change of the cavity caused by H₂ are

$$\Delta f_0 = K(\bar{C} - C_{\text{air}}) \approx \frac{n}{2 - 3n/2} K C_{\text{air}} \quad (2)$$

$$\Delta(\rho C) = \bar{\rho}\bar{C} - \rho_{\text{air}}C_{\text{air}} \approx n[(1 + n/2)\rho_{\text{H}_2} - \rho_{\text{air}}/2]C_{\text{air}}. \quad (3)$$

The resonance frequency shift Δf_0 and acoustic characteristic impedance change $\Delta(\rho C)$ are thus directly proportional to the H₂ concentration n when H₂ concentration n is a small quantity.

Suppose that the piezoelectric driving element is operated at a constant vibration velocity, which causes the gas particles to vibrate at a constant average speed v_e in the cavity. As a result, any change in the acoustic characteristic impedance, $\Delta(\rho C)$, will cause a change in acoustic intensity radiation (ΔI):

$$\Delta I = \Delta(\rho C)v_e^2. \quad (4)$$

[Note, $\Delta(\rho C)$ is a negative value because $\rho_{\text{H}_2} \ll \rho_{\text{air}}$.] According to Eq. (4), a cavity containing a gas of low acoustic impedance will result in a lower acoustic intensity radiation if the gas particles vibrate at a constant average speed v_e . Because the voltage signal V_s induced from the sensing element is $\sim \Delta I$ and $\Delta I \sim n$ [by Eqs. (3) and (4)], a small change in H₂ concentration n will produce a near linearly proportional change in V_s . Consequently, there exists a direct linear signal between the acoustic properties of the cavity and the H₂ concentration there within, which can be measured by the voltage output from a piezoelectric sensing element. The air acoustic speed and mass density are 330 m/s and 1.29 kg/m³, whereas these of H₂ are 1280 m/s and 0.089 kg/m³, respectively. This big difference in acoustic properties offers significant potential to detect changes in H₂ concentration with high sensitivity.

A PSRC prototype gas sensor with an operational frequency of 4.7 kHz was built, as shown in Fig. 1. This prototype consisted of two PZT thin layers with a diameter of 8 mm and a thickness of 100 microns, and a plastic cavity of 7 mm in diameter and 3 mm in height. An effective method to operate a PSRC sensor is at 90° or -90° phase state under constant frequency conditions. When H₂ enters the cavity, a phase shift, ΔP_s , of the resonance state will occur. H₂ also will result in an acoustic impedance change, which can be detected as a voltage change ΔV_s .

The response of the PSRC sensor to changes in H₂ concentration was determined in a H₂ test chamber. A small ac (4.794 kHz) voltage signal of 0.1 V_{rms} was used to drive a piezoelectric element at one end of the cavity. A lock-in amplifier was used to monitor the signal from the sensing element of the PSRC sensor. The temperature and relative humidity were held constant in the test chamber. To characterize the PSRC sensors capability of quantitative detection, the H₂ concentration in test chamber was varied over a wide concentration range from $10^{-6} < n < 0.2$.

Figures 2(a) and 2(b) show the sensor output phase angle and voltage for the PSRC prototype as a function of H₂ concentration. The H₂ concentration growth rate was held constant at $\Delta n/\Delta t = 0.091$ (ppm/sec). In Figs. 2(a) and 2(b),

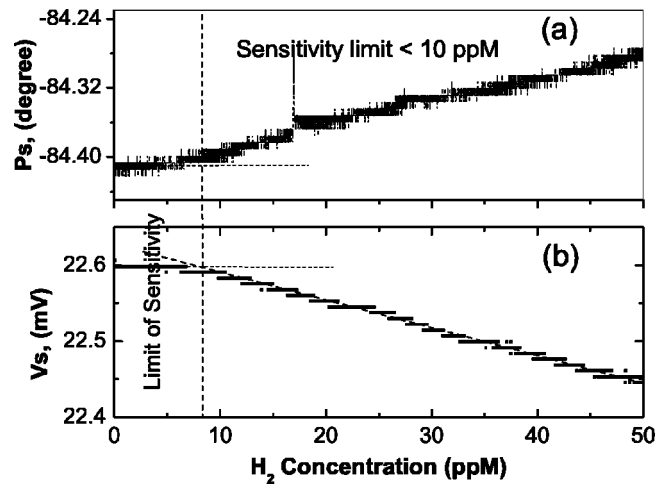


FIG. 2. PSRC sensor (a) phase and (b) voltage as a function of H₂ concentration at low concentration of H₂ (H₂ generation by electrochemical method). Constant circumstance temperature and humidity: 16 °C and 36%, respectively.

it can be seen that both the voltage and phase angle can detect changes in H₂ concentration of less than 10 ppm (~8 ppm). Above this sensitivity limit, the voltage and phase output were both found to be linear functions of H₂ concentration. For example, an H₂ concentration change of 42 ppm resulted in a phase shift of 0.113° and a voltage change of -0.16 mV. These correspond to relative changes of $\Delta P_s/P_{s0} = 1.34 \times 10^{-3}$ and $\Delta V_s/V_{s0} = -7.1 \times 10^{-3}$, where $P_{s0} = -84.412$ and $V_{s0} = 22.6$ mV.

The performance of the prototype PSRC sensor was evaluated over wider and higher H₂ concentration ranges: (i) 0–4000 ppm and (ii) 0%–10%. Figures 3(a) and 3(b) show the voltage and phase angle as a function of time over an intermediate H₂ concentration range. The concentration was increased by 670 ppm/step, using a total of six steps and a total H₂ concentration change of 4025 ppm. This resulted in a maximum total phase shift of 2.07° and a voltage change of -0.206 mV. The corresponding relative changes are

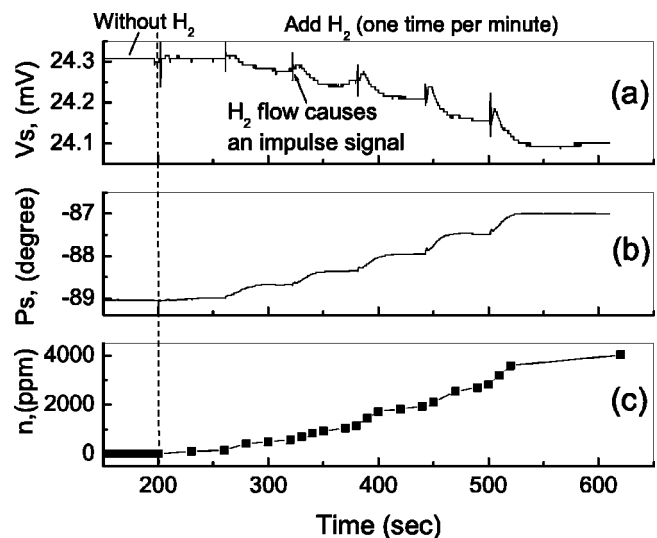


FIG. 3. Measurements in the H₂ concentration range of 0 to 4000 ppm: (a) voltage and (b) phase as a function of time for the PSRC sensor, (c) voltage as a function of time for the conventional ceramic gas sensor (Riken Keiki, Model SD-70). Constant circumstance temperature and humidity: 16 °C and 31%, respectively.

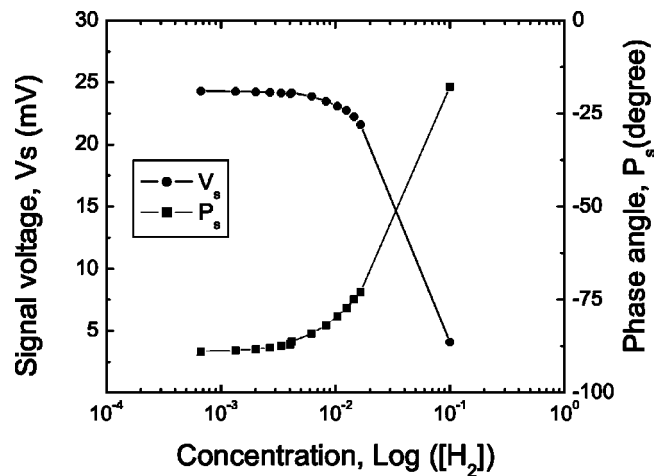


FIG. 4. Voltage and phase as a function of H_2 concentration for the PSRC sensor in the concentration range of $6 \times 10^{-4} < n < 0.2$. Constant circumstance temperature and humidity: 16 °C and 32%, respectively.

$\Delta P_s/P_{s0} = 2.32 \times 10^{-2}$ and $\Delta V_s/V_{s0} = -8.48 \times 10^{-3}$, where $P_{s0} = -89.06^\circ$ and $V_{s0} = 24.30$ mV. The various impulse signals in Fig. 3(a) are due to the step-wise manner in which the H_2 concentration was increased. Figure 3(c) shows the H_2 concentration as a function of time, determined using a conventional semiconducting ceramic sensor. Even though H_2 was introduced into the test chamber in a step-wise manner, its time-dependent response was smooth. This reflects the fact that its response time is significantly longer than the time differential between steps in the H_2 concentration.

Figure 4 shows the voltage and phase angle as a function of H_2 concentration. The voltage and phase angle can be seen to be proportional to the H_2 concentration over a wide concentration range of $6 \times 10^{-4} < n < 0.1$. This resulted in a maximum total phase shift of $\sim 75^\circ$ and a voltage change of ~ -20 mV. (As a comparison, the semiconductor ceramic sensor became saturated and its voltage independent of H_2 concentration for $n \geq 8.3 \times 10^{-3}$). Theoretically, the gas in the cavity may be H_2 of 100%. The response time of the PSRC sensor to H_2 concentration changes was very rapid; typically, it is about 1.5 s (see Fig. 5). Note, the cavity of PSRC sensor should be kept at a constant temperature and humidity condition, as it is also sensitive to these variations.

In conclusion, we have demonstrated a PSRC concept in H_2 sensing which uses sound resonance and acoustic property differences of gases as a sensing mechanism. It is a compact, robust, and light weight sensor. It has very low working voltages (< 100 mV) and extremely low-power consumptions ($< 100 \mu\text{W}$). Investigations of a PSRC prototype have demonstrated a sensitivity limit of 8 ppm, a fast response time ~ 1.5 second, and a signal (phase and voltage) that is a linear function of H_2 concentration in the low con-

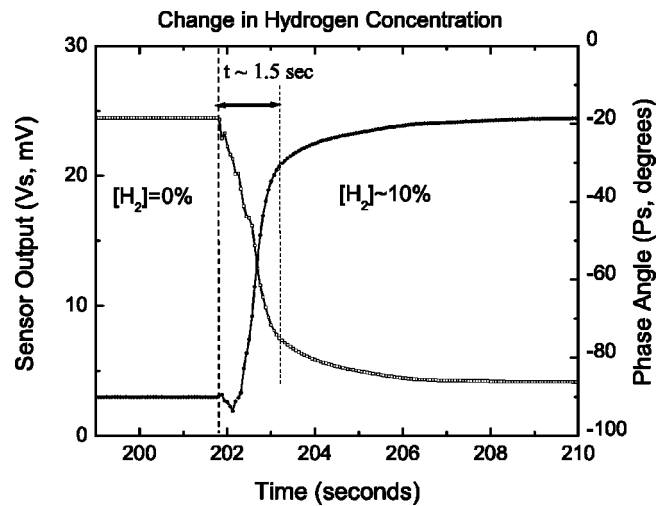


FIG. 5. Illustration of response time of PSRC sensor to a change in H_2 concentration.

centration range, and that is also proportional to H_2 concentration over a wide range of H_2 concentrations between $8 \times 10^{-6} < n < 0.2$.

This research was supported by the NASA, Marshall Space Flight Center. Any opinions, findings, and conclusions or recommendations expressed in this material are those of the author(s) and do not necessarily reflect the views of NASA.

- ¹D. D. Lee and D. S. Lee, *IEEE Sensors J.* **1**, 3 (2001).
- ²K. Ihokura and J. Watson, *The Stannic Oxide Gas Sensors* (CRC Press, Boca Raton, 1994).
- ³D. D. Lee, *Chem. Sens. Technol.* **5**, 79 (1994).
- ⁴C. Xu, J. Tamaki, and N. Yamazoe, *J. Mater. Sci.* **27**, 963 (1992).
- ⁵W. Weppner, *Proceedings of the Second International Meeting on Chemical Sensors*, Bordeaux, France, 1986, p. 59.
- ⁶A. D. John, *Analytical Chemistry Handbook* (McGraw-Hill, New York, 1995).
- ⁷M. J. C. Petty and R. Casalini, *Eng. Sci. Edu. J.* **99**, (2001).
- ⁸R. Casalini, J. Nagel, U. Oertel, and M. C. Petty, *J. Phys. D* **31**, 3146 (1998).
- ⁹S. L. Firebaugh, K. F. Jensen, and M. A. Schmidt, *J. Microelectromech. Syst.* **10**, 232 (2001).
- ¹⁰M. A. Butler, *Appl. Phys. Lett.* **45**, 1007 (1984).
- ¹¹I. D. Avramov, S. Kurosawa, M. Rapp, P. Krawczak, and E. I. Radeva, *IEEE Trans. Microwave Theory Tech.* **49**, 827 (2001).
- ¹²I. A. Ges and B. A. Budkevich, *Proceedings of the 1999 Joint Meeting EFTF-IEEE IFCS*, 1999, p. 1070.
- ¹³F. Favier, E. C. Walter, M. P. Zach, T. Benter, and R. M. Penner, *Science* **21**, 2227 (2001).
- ¹⁴H. I. Chen, Y. I. Chou, and C. Y. Chu, *Sens. Actuators B* **85**, 10 (2002).
- ¹⁵S. V. Slobodchikov, D. N. Goryachev, K. M. Salikhov, and O. M. Sreseli, *Semiconductors* **33**, 339 (1999).
- ¹⁶W. P. Kang and Y. Gurbuz, *J. Appl. Phys.* **75**, 8175 (1994).
- ¹⁷W. C. Liu, H. J. Pan, H. I. Chen, K. W. Lin, S. Y. Cheng, and K. H. Yu, *IEEE Trans. Electron Devices* **48**, 1938 (2001).
- ¹⁸R. T. Muehleisen, *ARLO* **3**, 118 (2002).
- ¹⁹E. R. Braga, A. Y. Nakano, and M. P. Cunha, *Proceedings of the S BMO/ IEEE M TT-S IMOC'99*, 1999, p. 342.